# Gold nanoparticles film for Q-switched pulse generation in thulium doped fiber laser cavity*

**Ahmad H. A. Rosol[1], Afiq A. A. Jafry[2], Norrima Mokhtar[1], Moh Yasin[3], and Sulaiman Wadi Harun[1]****
*1. Department of Electrical Engineering, University of Malaya, Kuala Lumpur 50603, Malaysia*
*2. Department of Physics, Faculty of Science, Universiti Teknologi Malaysia, Skudai 81310, Malaysia*
*3. Department of Physics, Faculty of Science and Technology, Airlangga University, Surabaya, Indonesia*

(Received 14 November 2020; Revised 21 December 2020)


Passively Q-switched thulium doped fiber laser (TDFL) has been successfully demonstrated using gold nanoparticles (GNPs), which were embedded into polyvinyl alcohol as saturable absorber (SA). The stable self-starting Q-switched laser was generated to operate at 1 891 nm when a tiny piece of the prepared film was slot in between two fiber ferrules and incorporated into the laser cavity. The repetition rate can be adjusted from 48.54 kHz to 49.64 kHz while the pulse width decreased from 3.52 μs to 2.38 μs with the increase of 1 550 nm pump power from 840 mW to 930 mW. The corresponding pump power output power linearly increased from 3.62 mW to 6.3 mW with a slope efficiency of 2.53%. The maximum peak power and pulse energy were recorded at about 39 mW and 0.12 μJ, respectively at pump power of 930 mW. The Q-switching operation was caused by the surface plasmon resonance absorption of GNPs.
**Document code:** A **Article ID:** 1673-1905(2021)08-0449-5
**DOI** https://doi.org/10.1007/s11801-021-0180-9

Fiber laser technology has obtained significant interests for many researchers because of their robustness, compact in size and easy to handle compared to the bulk laser[1]. The laser can be realized by using either the erbium-, ytterbium- or thulium-doped fiber as active medium for operations in wavelength regions of 1.55 μm, 1.0 μm or 2.0 μm, respectively[2,3]. thulium-doped fiber laser (TDFL) has gained more interests because of their advantages for application in variety of fields such as military, remote sensing, spectroscopy and medical[4,5]. In addition, the TDFL operates in eye-safe wavelength region that suite for free space applications such as light detection and ranging (LIDAR) and telecommunication systems. On the other hand, 2 μm lasers are more efficient in absorbing liquid compared to other operating wavelengths of 1.0 μm and 1.55 μm and thus they are more favorable for use in medical treatment[4,6,7].

Q-switching in TDFL cavity can be realized by either active or passive method. In comparison with the passive, active technique requires extra optical modulator to modulate the propagating light for pulse generation. Moreover, it is bulky in size, complex to fabricate and quite costly. But the passive technique based on saturable absorber (SA) is simpler in fabrication, smaller in size, inexpensive and more efficient for implementation in generating Q-switched fiber laser. Up to date, many materials have been examined and reported as SA such as semiconductor saturable absorber mirror (SESAM), graphene and black phosphoros[8-10]. SESAM is one of the earlier SA, which was widely used in realizing Q-switched fiber laser since it was firstly discovered in 1990s. Nevertheless, the fabrication of SESAM is complex and quite expensive. Graphene SA has also been used for generating Q-switched laser due to its ability to operate in a broader wavelength region. It has obtained more attentions in the past years since it is relatively cheaper than SESAM while exhibiting a lower saturation intensity. However, this type of SA shows a significantly lower modulation depth (2.3%) per layer[11]. BP shows the tendency to change its optical properties when it exposed to the air molecule. Moreover, it is quite difficult to integrate the BP material into the fiber laser cavity since it requires a unique arrangement and packaging to prevent its exposure to air molecules[12]. On the other hand, carbon nanotube, topological insulator, transition metal dichalcogenide and transition metal oxide based SAs have also gained great attention for Q-switched pulse generation[13-15]. These materials have a good nonlinear optical response especially in the infra-red region.

Metal nanoparticles are also drawing much interests in recent years for SA applications due to their high nonlinear optical response, the high plasmonic effect of their surface and fast response time[16,17]. For example, silver nanoparticle has been used as passive SA for generating Q-switched erbium-doped fiber laser (EDFL)[18]. Moreover, Muhammad et al have demonstrated a Q-switching operation in C-band region

* This work has been supported by the University of Malaya (No.ML001-2017B).
** E-mail: swharun@um.edu.my

using a copper (CuNP) base[19]. However, insufficient attention was paid to gold nanoparticles (GNPs) for the Q-switching application even though it has shown the promising properties. GNPs have excellent nonlinear properties and thus is suitable for the SA application by making use of their surface plasmon resonance (SPR) effect. In this paper, Q-switched fiber laser is demonstrated for the first time using GNPs film in the TDFL cavity to operate in 2 μm region. A stable pulse train with the maximum repetition rate of 49.64 kHz, minimum pulse width of 2.38 μs and highest energy of 0.12 μJ was obtained. The finding shows that GNPs could be a promising candidate for various photonic applications especially for operation in near and mid-IR bands.

The ingredients for GNPs synthesization consist of gold (III) chloride trihydrate (50% Au basis) ($HAuCl_4$), tri-sodium citrate ($Na_3C_6H_5O_7$, TSC), poly(sodium 4-styrenesulfonate) (PSSS), and sodium borohydrate ($NaBH_4$). The GNPs was prepared in a fume hood so that the reaction occurs in a non-toxic environment with limited specks of dust and water vapor. First, the mixture of 50 mL TSC, 3 mL PSSS and 3 mL of $NaBH_4$ were stirred in a beaker with 1 L deionized (DI) water at 450 rpm. Next, 50 mL of $HAuCl_4$ was carefully added using syringe (2 mL/min), followed by 20 mL of excess TSC. The solution was dried for 5 min and undergone centrifugation afterward. The GNPs was stirred to mix with polyvinyl alcohol (PVA). PVA powder (purchased from Sigma Aldrich) was dissolved in 80 mL of DI water and stirred for 2 h at 145 °C. We used PVA as a host polymer to ease the incorporation of GNPs into the laser cavity while protecting the material from environmental disturbances such as humidity and oxidation. The as-prepared solution was poured onto a petri dish, left to dry for 48 h and carefully peeled later. Field emission scanning electron microscopy (FESEM) image was captured. The morphological mapping of the as-prepared GNPs PVA was displayed in Fig.1(a) with the magnification of 1 000 times within a 10 μm dimension. The circle image shows the fiber ferule fully cover with the GNPs PVA film. The nonlinear transmission properties of GNPs was investigated and tabulated in Fig.1(b). Collected data were fitted using the following equation:

$$T(I)=1-\Delta T\times\exp\left(-I/I_{sat}\right)-T_{ns}\ , \quad (1)$$

where $T(I)$ is an intensity-dependent transmission coefficient, $\Delta T$ is a modulation depth, $T_{ns}$ is a non-saturable loss, $I$ is an input intensity, and $I_{sat}$ is a saturable intensity. We obtained a modulation depth of 13.6%, a non-saturable loss of 48%, and a saturable intensity of 0.05 MW/cm$^2$. Fig.1(c) shows the linear absorption profile of the GNPs film within a wavelength range from 1 890 nm to 1 950 nm. The film has an absorption loss of about 3.2 dB at 1 891 nm.

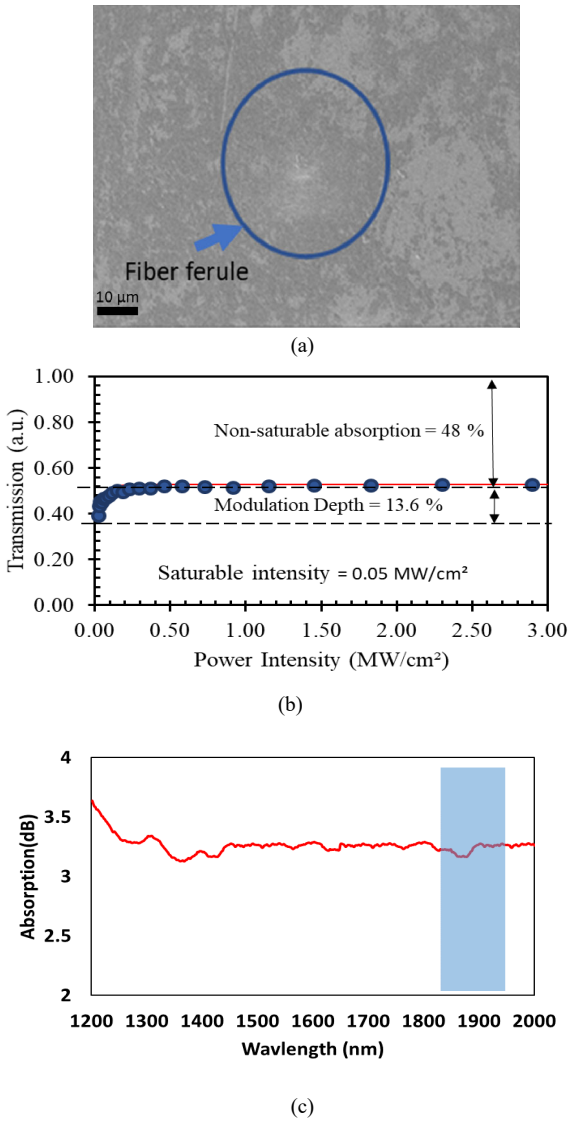


**Fig.1 (a) The SEM image of the film with the illustration of fiber ferrule on top of the image; (b) The nonlinear optical profile for the GNPs film; (c) The linear absorption of the GNPs film**

Fig.2 illustrates the configuration of the proposed Q-switched TDFL using the prepared GNPs based SA. The cavity employed a homemade fiber laser operating at 1 550 nm as a pump light source to pump the active medium, 5-m-long commercial thulium doped fiber (TDF, Nufern SM-TSF-9/125). The pump was launched into the TDF through a 1 550/2 000 nm wavelength division multiplexer (WDM). The TDF has a core and cladding diamater of 9 μm and 125 μm, respectively while the numerical apature is 0.15. The absorption of thulium ion of the fiber are 27.0 dB/m and 9.3 dB/m at 793 nm and 1 180 nm, respectively. The dispersions of the SMF-28 fiber and the thulium doped fiber at 1.9 μm are −86.8 ps$^2$km$^{-1}$ and −12 ps$^2$ km$^{-1}$, respectively. Thus the total net normal cavity dispersion is estimated to be ~0.53 ps$^2$. The total cavity length is 13 m. A 90:10 output coupler was used to tap 10% of the ring cavity for

measurement while allowing the remaining 90% of the light to continuously oscillate in the cavity. The 10% output was connected to various optical measurement equipments such as optical spectrum analyzer (OSA, YOKOGAWA AQ6375), a 500 MHz digital oscilloscope and 7.8 GHz of radio frequency spectrum analyzer (RFSA, Anritsu). The OSA was used to measure the output spectrum of the laser. Oscilloscope and RFSA were used for analyzing the generated pulse train in time and frequency domain, respectively. A fast photodetector was used for both oscilloscope and RF as a bridge to transfer the light from the fiber cavity to those equipments. A tiny piece of GNPs film was adhered onto the fiber ferule and then sandwiched with another fiber ferrule to form a SA device as depicted in Fig.2. The SA was incorporated into the cavity between the 90% port of output coupler and the input port port of WDM. It is noted that an index matching gel was pre-applied on the ferrules' surface to minimize unwanted reflection during lasing.

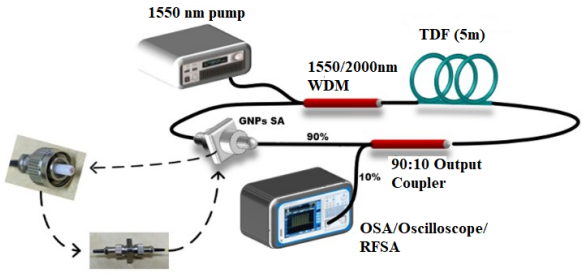


**Fig.2 The illustration of the proposed Q-switched TDFL cavity**

The performance of the TDFL without inserting the GNPs SA was firstly investigated. The TDFL produced continuous wave (CW) laser at a threshold pump power of 760 mW. After incorporating the GNPs film into the TDFL cavity, a stable Q-switched pulse train was succesfully generated at a pump power of 840 mW. Fig.3(a) compares the output spectral characteristic of the TDFL with and without the SA at the threshold pump power. The central wavelength was 1 884 nm and 1 891 nm for the CW and Q-switched operation, which was obtained without and with the insertion of GNPs SA, respectively. The 4 nm shifting of the wavelength to the shorter wavelength was observed when incorporating the GNPs film into the cavity. This is attributted to the increase of cavity loss when the film was integrated into the cavity. The laser operational wavelength shifts to shorter wavelength to acquire additional gain to compensate for the loss. The spectrum of 790 mW of pump power also represent in the figure. The peak of spectrum at 790 mW pump power shows a slightly increase due to the high gain in the cavity. Fig.3(b) depicts the typical oscilloscope trace of pulses train at the maximum pump power of 930 mW. The emerging of the Q-switched pulse train from the cavity is attributted to the longitudinal SPR absorption of GNPs. This is attributed to the metal nanoparticles have close-lying bands that permits the electron to move freely. The energy filled the electron on the conduction until it stimulated the resonance band of plasmon to the surface as the light beam reaches the gold particles[20]. The SPR effect modulates the cavity loss to generate the Q-switched pulses[21]. The peak-to-peak duration was observed to be about 20.60 μs corresponding to the repetition rate of 48.54 kHz as depicts in Fig.3(b). The single pulse width was measured to be ~2.38 μs as shows in Fig.3(c).

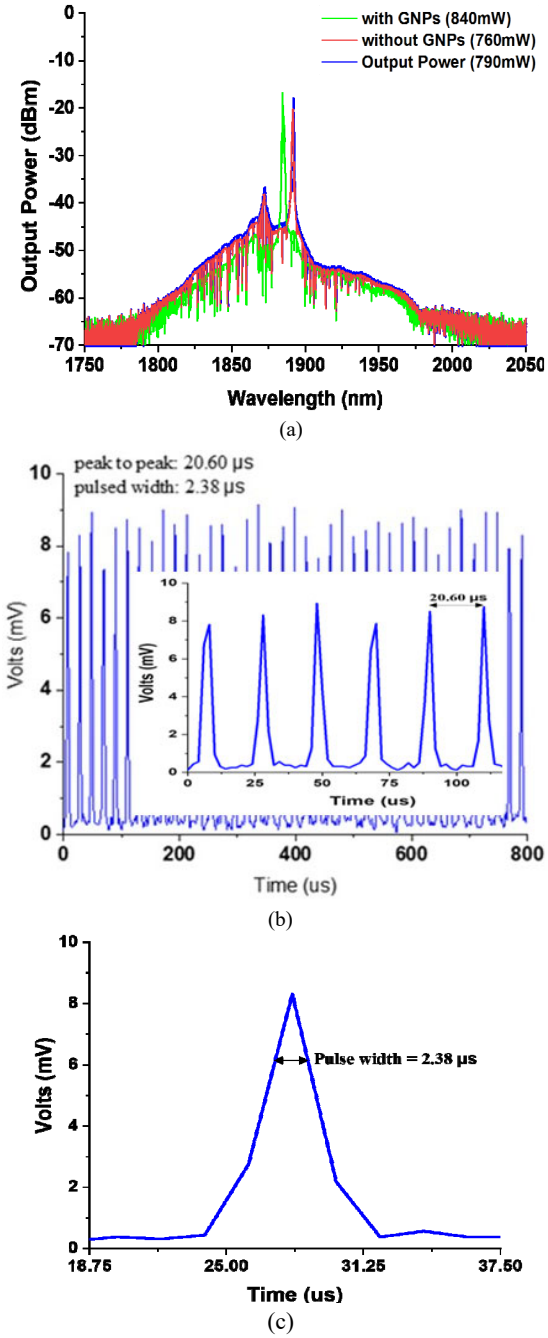


**Fig.3 Spectral and temporal characteristics of the GNPs based Q-switched TDFL: (a) Spectral characteristics with and without SA; (b) Pulse train at the pump power of 930 mW with the peak-to-peak interval of 20.60 μs; (c) The single pulse envelop with a pulse width of 2.38 μs**

Fig.4(a) presented the relationship between both repetition rate and pulse width parameters and the pump power. By adjusting the pump power from 840 mW to 930 mW, the repetition rate increased from 48.54 kHz to 49.64 kHz while the pulse width had a shrinking trend from 3.52 μs to 2.38 μs. This trend is typical for passive Q-switched fiber lasers[22,23]. Fig.4(b) shows a nearly linear increasing trend of the average output power, peak power, and pulse energy with the pump power. When the 1 550 nm laser power was raised from 840 mW to 930 mW, the average output power increased linearly from 3.62 mW to 6.3 mW. The slope efficiency represents the optical-to-optical efficiency of the GNPs based Q-switched TDFL. The efficiency was calculated to be about 2.53%, which is relatively low. This is most probably due to the use of 10 dB output coupler, which allowed only 10% of the oscillating laser to be extracted from the cavity. The laser efficiency could be enhanced by increasing the output ratio of the coupler. The output efficiency could also be improved by minimizing the insertion loss induced by the SA and optimizing the cavity design by reducing the splicing loss and fiber length. At 930 mW pump power, the maximum peak power and pulse energy were recorded at about 39 mW and 0.12 μJ, respectively.

The proposed SA should have a long term stability for use in various practical applications. Fig.5 plots the RF spectrum of the Q-switched TDFL at 840 mW pump power, it was measured by using a high resolution RF spectrum analyzer. The first harmonic of RF spectrum was obtained at 48.54 kHz with a signal-to-noise ratio (*SNR*) of approximately 70 dB, which indicates an excellent and stable Q-switched performance in the proposed TDFL configuration. The resolution of the frequency spectrum is 10 kHz. If the pump power further increased above 930 mW, the Q-switched laser will become unstable. However, the optical damage threshold of GNPs SA was obseved to be greater than 2 000 mW The performance of GNP is comparable with other SAs based on 2D materials as shown in Tab.1. The mode-locked pulses cannot be generated in the current cavity even though the pump power was varied within a wide range. However, the mode-locked pulses could be realized with further optimization of cavity design and SA to reduce their loss and increase the nonlinearity characteristic.

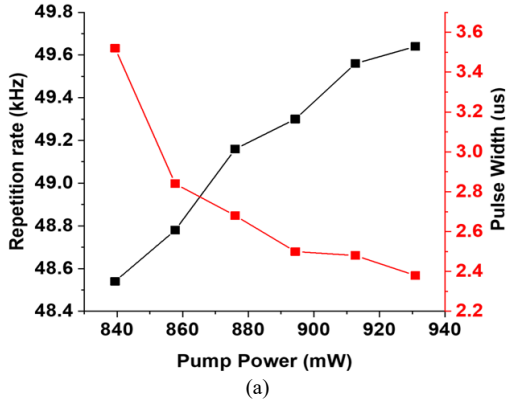


(a)

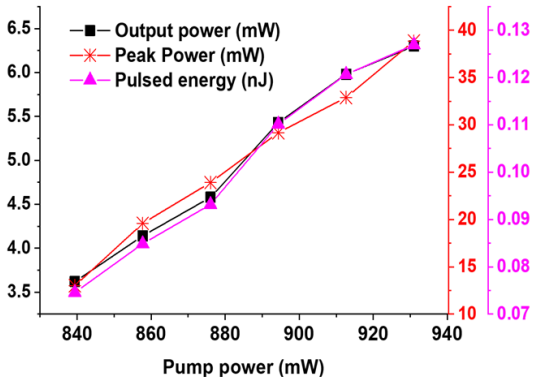


(b)

**Fig.4 Q-switching performance against pump power: (a) Repetition rate and pulse width; (b) Average output power, peak power and pulse energy**

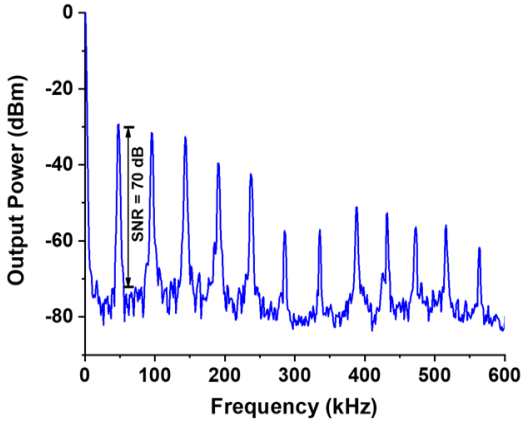


**Fig.5 RF spectrum with the fundamental repetition rate of 48 kHz and *SNR* of 70 dB**

**Tab.1 Q-switching performance for various SAs operating in TDFL cavity**

| SA | Wavelength (nm) | Pulse width (μs) | Repetition rate (kHz) | Max. energy (uJ) | Ref. |
|---|---|---|---|---|---|
| $MoSe_2$ | 1 924 | 2.50—1.76 | 33.60—48.10 | 1 | [24] |
| $TiO_2$ | 1 935 | 3.91—1.91 | 30.12—36.96 | 0.3 | [25] |
| $MoO_{3-x}$ | 1 910 | 8.2—1.6 | 24.3—60.1 | 0.15 | [26] |
| GNPs | 1 891 | 3.52—2.38 | 48.54—49.64 | 0.12 | This work |

In conclusion, a new SA based on GNPs has been successfully developed for realizing an all-fiber passively Q-switched TDFL. The SA was inserted into a ring laser cavity to produce a stable pulse train operating at center wavelength of 1 891 nm. As the pump power adjusted from 840 mW to 930 mW, the repetition rate and pulse width of the laser can be tuned from 48.54 kHz to 49.64 kHz and 3.52 μs to 2.38 μs, respectively. The maximum average output power, peak power and pulse

energy were recorded at about 6.3 mW, 39 mW and 0.12 μJ, respectively at 930 mW pump power. The result indicates that GNPs has a good nonlinearity and thus is suitable for use in various photonic devices operating in 2 μm region.

## References


[1] N. Nishizawa, Japanese Journal of Applied Physics **53**, 090101 (2014).

[2] Y Zhou, R Zhang, P Chen, Y Liu, Y Fang, T Wang, X Li, P Kuan and M Liao, Laser Phys. **29**, 055101 (2019).

[3] RI Woodward, RCT Howe, TH Runcorn, G Hu, F Torrisi, EJR Kelleher and T Hasan, Optics Express **23**, 20051 (2015).

[4] Maciej Janeczek, Jacek Świderski, Albert Czerski, Bogusława Żywicka, Jolanta Bujok, Maria Szymonowicz, Ewa Bilewicz, Maciej Dobrzyński, Mariusz Korczyński, Aleksander Chrószcz and Zbigniew Rybak, Preliminary Evaluation of Thulium Doped Fiber Laser in Pig Model of Liver Surgery, BioMed Research International, 2018.

[5] Z. Qu, Q. Li, H. Meng, X. Sui, H. Zhang and X. Zhai, Application and the Key Technology on High Power Fiber-Optic Laser in Laser Weapon, International Symposium on Optoelectronic Technology and Application 2014: International Society for Optics and Photonics, 92940C (2014).

[6] M. Michalska, W. Brojek, Z. Rybak, P. Sznelewski, M. Mamajek and J. J. L. P. L. Swiderski, Laser Phys. Lett. **13**, 115101 (2016).

[7] O. Traxer and E. X. Keller, Thulium Fiber Laser: the New Player for Kidney Stone Treatment? A Comparison with Holmium: YAG laser, World Journal of Urology, 1 (2019).

[8] H.-Y. Wang, W.-C. Xu, A.-P. Luo, J.-L. Dong, W.-J. Cao and L.-Y. Wang, Optics Communications **285**, 1905 (2012).

[9] Qiaoliang Bao, Han Zhang,Yu Wang, Zhenhua Ni, Yongli Yan, Ze Xiang Shen, Kian Ping Loh and Ding Yuan Tang, Advanced Functional Materials **19**, 3077 (2009).

[10] M. Buscema, D. J. Groenendijk, G. A. Steele, H. S. Van Der Zant and A. Castellanos-Gomez, Nature Communication **5**, 1 (2014).

[11] ZQ Luo, M Zhou, J Weng, GM Huang, HY Xu, CC Ye and ZP Cai, Optics Letters **35**, 3709 (2010).

[12] Wood Joshua D., Wells Spencer A., Jariwala Deep, Chen Kan-Sheng, Cho EunKyung, Sangwan Vinod K., Liu Xiaolong, Lauhon Lincoln J., Marks Tobin J. and Hersam Mark C, Nano Letters **14**, 6964 (2014).

[13] S. Y. Set, H. Yaguchi, Y. Tanaka and M. Jablonski, IEEE Journal of Selected Topics in Quantum Electronics **10**, 137 (2004).

[14] P Yan, R Lin, S Ruan, A Liu, C Hao, Y Zheng, S Chen, C Guo and J Hu, Scientific Report **5**, 8690 (2015).

[15] Wang Kangpeng, Wang Jun, Fan Jintai, Lotya Mustafa, O'Neill Arlene, Fox Daniel, Feng Yanyan, Zhang Xiaoyan, Jiang Benxue and Zhao Quanzhong, ACS Nano **7**, 9260 (2013).

[16] Tao Jiang, Yang Xu, Qijun Tian, Lai Liu and Zhe Kang, Applied Phys. Lett. **101**, 151122 (2012).

[17] Xu-De Wang, Zhi-Chao Luo, Hao Liu, Nian Zhao, Meng Liu, Yan-Fang Zhu, Jian-Ping Xue, Ai-Ping Luo and Wen-Cheng Xu, Opt. Commun. **346**, 21 (2015).

[18] H Guo, M Feng, F Song, H Li, A Ren, X Wei, Y Li, X Xu and J Tian, IEEE Photon. Technol. Lett. **28**, 135 (2015).

[19] A. R. Muhammad, M. T. Ahmad, R. Zakaria, H. R. A. Rahim, S. F. A. Z. Yusoff, K. S. Hamdan, H. H. M. Yusof, H. Arof and S. W. Harun, Chinese Phys. Lett. **34**, 034205 (2017).

[20] U Gurudas, E Brooks, DM Bubb, S Heiroth and T Lippert, Journal of Applied Physics **104**, 073107 (2008).

[21] M Na, S Tao, W Yang, Q Chen and H Zhang, Optics Express **26**, 9017 (2018).

[22] M. Ahmad, A. Muhammad, R. Zakaria, H. Ahmad and S. W. Harun, Optik **207**, 164455 (2020).

[23] S Li, Z Kang, N Li, H Jia and G Qin, Optical Materials Express **9**, 2406 (2019).

[24] Z Luo, Y Huang, Z Min, Y Li and J Weng, Journal of Lightwave Technology **32**, 4077 (2014).

[25] Latiff A. A., Rusdi M. F. M., Hisyam M. B., Ahmad H. and Harun S. W., Journal of Modern Optics **64**, 187 (2017).

[26] Wang M., Huang S., Zeng Y. J., Yang J., Pei J. and Ruan S., Optical Materials Express **9**, 4429 (2019).